http://dx.doi.org/10.5012/bkcs.2014.35.6.1732

Facile Preparation of Water Dispersible Red Fluorescent Organic Nanoparticles for Cell Imaging

Miao Luo

College of Basic Education, Zhanjiang Normal University, Zhanjiang, 524037, Guangdong, China
E-mail: luomiao1104@126.com
Received January 14, 2014, Accepted February 18, 2014

Red fluorescent organic nanopaticles (FONs) based on a diarylacrylonitrile derivative conjugated molecule were facilely prepared by surfactant modification. Such red FONs showed excellent water solubility and biocompatibility, making them promising for cell imaging applications.

Key Words : Red fluorescent organic nanopaticles, Diarylacrylonitrile derivative, Surfactant modification, Anti-aggregation-caused quenching effect, Cell imaging

Introduction

Optical bioimaging is one of the rapid growing areas in biological and biomedical research.[1] Fluorescence cellular probes with red/near-infrared (R/NIR, > 600 nm) emission are highly desirable for biological applications due to their low optical absorption and autofluorescence of biological media.[2-4] Up to date, various fluorescent materials including organic dyes,[5-7] fluorescent proteins,[8] fluorescent inorganic nanoparticles (NPs) [9-14] have been used as R/NIR probes. However, many of these fluorescent materials often suffered from obvious disadvantages such as water insolubility, photobleaching and toxicity, which severely limited their practical bioimaging applications. For example, most of organic dyes are intrinsic hydrophobic and instable in biological media.[15] Usage of fluorescent proteins is often limited due to the high cost, low molar absorptivity and low photobleaching thresholds,[16] while inorganic NPs or quantum dots are non-biodegradable and often toxic to living organisms.[17-19] Compared with the fluorescent bioprobes currently available, organic nanoparticles (FONs) are receiving more and more attentions due to flexible synthetic approaches of these small organic molecules and their biodegradation potential.[20-24] Because of these virtues, various FONs including fluorescent conjugated polymers, polydopamine nanoparticles and aggregation-induced-emission (AIE), or aggregation induced emission enhancement (AIEE) materials have been reported in recent years.[25-31] Among them, the AIE or AIEE based FONs have attracted great research interest because they could overcome the notorious aggregation-caused quenching (ACQ) effect of most organic dyes. Different AIE or AIEE units such as siloles,[32-34] cyano-substituted diarylethene,[35-39] tetraphenylethene,[40-43] triphenylethene,[44-48] distyrylanthracene derivatives[49-53] conjugated molecules have been examined for chemosensors and bioimaging applications.

However, direct employment of AIE or AIEE based FONs for bioimaging has been proven problematic due to the strong hydrophobicity of most of AIE or AIEE units. The introduction of charges into AIE (or AIEE) materials may improve their solubility in aqueous media, but the electric charges of the highly concentrated ionized dyes would affect intracellular physiology and sometimes even kill the cells.[54] Therefore, facile preparation of novel FONs which exhibited enhanced water dispersibility, excellent biocompatibility and photoluminescent properties simultaneously is of great significance.

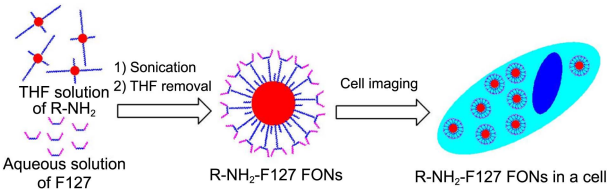

Scheme 1. The formation of hydrophilic red FONs.

In this connection, it has to be noted that Zhang *et al.* had earlier reported facile transformation of hydrophobic AIE (**An18**) into hydrophilic FONs by mixing the unit with a commercial surfactant pluronic F127.[55] The FONs thus formed reveal not only high water solubility but also excellent biocompatibility-a promising observation for cell imaging applications. One drawback, however, of these AIE-based FONs for bioimaging lies in the fact that their emission maxima fall in the range 530-550 nm, where interference with the body optical absorption, light scattering, and autofluorescence of biological media is unavoidable.

Herein, we report a facile method for the preparation of hydrophilic red FONs based on a diarylacrylonitrile derivative (**R-NH$_2$**) by surfactant modification (Scheme 1). The hydrophobic **R-NH$_2$** was changed to hydrophilic by surrounding with F127 to form **R-NH$_2$-F127** FONs, which exhibit good water dispersibility and anti-ACQ property. To exploit the potential biomedical applications of such red FONs (**R-NH$_2$-F127**), their biocompatibility as well as cell imaging applications were further investigated.

Experimental

Materials and Measurements. Thiophene, 3-(bromometh-

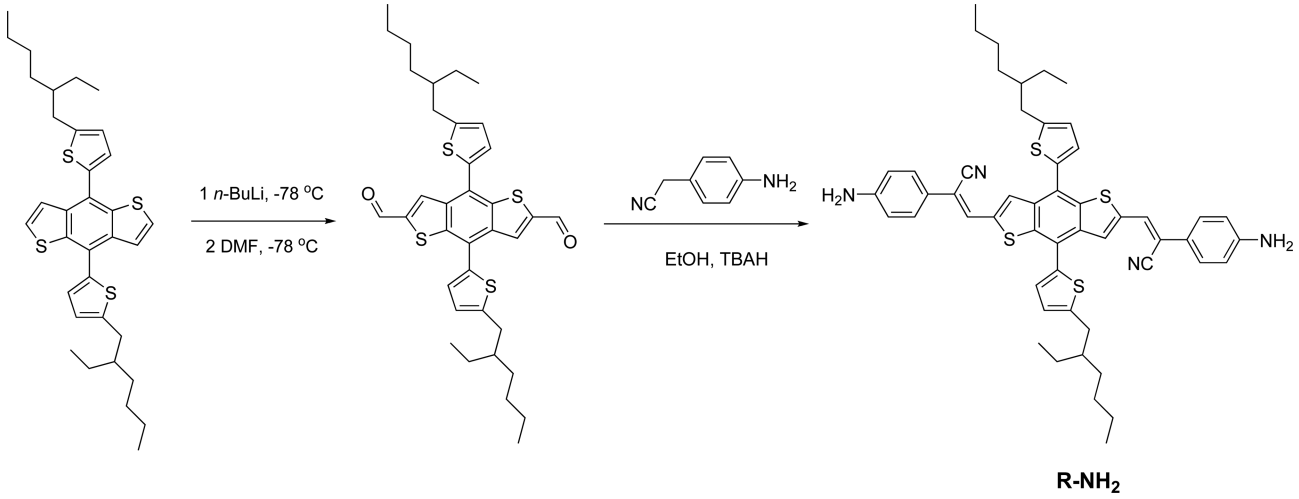

Scheme 2. Synthetic route of **R-NH$_2$**.

yl)heptane, thiophene-2-carboxylic acid, thionyl chloride, dimethylamine, *n*-butyllithium, stannic chloride, 2-(4-aminophenyl)acetonitrile, tetrabutylammonium hydroxide (0.8 M in methanol) purchased from Alfa Aesar were used as received. All other agents and solvents purchased from commercial sources were used directly without further purification. The synthetic route of **R-NH$_2$** was showed in Scheme 2, which was prepared according to the previous literature method.[56] Its structure was characterized and confirmed by standard spectroscopic methods.

Fluorescence spectra were measured on a PE LS-55 spectrometer with a slit width of 3 nm for both excitation and emission. Transmission electron microscopy (TEM) images were recorded on a JEM-1200EX microscope operated at 100 kV, the TEM specimens were made by placing a drop of the nanoparticles suspension on a carbon-coated copper grid. The FT-IR spectra were obtained in a transmission mode on a Perkin-Elmer Spectrum 100 spectrometer (Waltham, MA, USA). Typically, 8 scans at a resolution of 1 cm^{-1} were accumulated to obtain one spectrum. The size distributions measurement of the FONs in phosphate buffer solution (PBS) were determined using a zeta Plus apparatus (ZetaPlus, Brookhaven Instruments, Holtsville, NY).

Preparation of R-NH$_2$-F127 FONs. The preparation of **R-NH$_2$-F127** FONs was carried out as follows. Approximately 5 mg of synthesized dyes (**R-NH$_2$**) was dissolved in 20 mL of THF and then added dropwise into the solution of Pluronic F127 (20 mg) in 20 mL of H_2O in a 100 mL vial under sonication. And then the mixture was evaporated to remove the organic agent (THF) completely on a rotary evaporator at 40 °C. To remove the excess Pluronic F127, the **R-NH$_2$-F127** water dispersion was treated by repeated centrifugal washing process for three times.

Cytotoxicity of R-NH$_2$-F127 FONs. Cell morphology was observed to examine the effects of **R-NH$_2$-F127** FONs to A549 cells. Briefly, cells were seeded in 6-well microplates at a density of 1 × 10^5 cells mL^{-1} in 2 mL of respective media containing 10% FBS. After cell attachment, the plates were washed with PBS and the cells were treated with complete cell culture medium, or different concentrations of fluoridated **R-NH$_2$-F127** FONs prepared in 10% FBS containing media for 24 h. Then all samples were washed with PBS three times to remove the uninternalized FONs. The morphology of cells was observed by using an optical microscopy (Leica, Germany), the overall magnification was × 100.

The cell viability of **R-NH$_2$-F127** FONs on A549 cells was evaluated by cell counting kit-8 (CCK-8) assay. Briefly, cells were seeded in 96-well microplates at a density of 5 × 10^4 cells mL^{-1} in 160 μL of respective media containing 10% FBS. After cell attachment for 24 h, the cells were incubated with 10, 20, 40, 80, 120 μg mL^{-1} **R-NH$_2$-F127** FONs for 8 and 24 h, respectively. Then nanoparticles were removed and cells were washed with PBS for three times. 10 μL of CCK-8 dye and 100 μL of DMEM cell culture medium were added to each well and incubated for 2 h at 37 °C. Plates were then analyzed with a microplate reader (VictorIII, Perkin-Elmer). Measurements of formazan dye absorbance were carried out at 450 nm, with the reference wavelength at 620 nm. The values were proportional to the number of live cells. The percent reduction of CCK-8 dye was compared to controls (cells not exposed to **R-NH$_2$-F127** FONs), which represented 100% CCK-8 reduction. Three replicate wells were used per microplate, and the experiment was repeated for three times. Cell survival was expressed as absorbance relative to that of untreated controls. Results are presented as mean ± standard deviation (SD).

Confocal Microscopic Imaging of Cells using R-NH$_2$-F127 FONs. A549 cells were cultured in Dulbecco's modified eagle medium (DMEM) supplemented with 10% heat-inactivated fetal bovine serum (FBS), 2 mM glutamine, 100 U mL^{-1} penicillin, and 100 μg mL^{-1} of streptomycin. Cell culture was maintained at 37 °C in a humidified condition of 95% air and 5% CO_2 in culture medium. Culture medium was changed every three days for maintaining the exponential growth of the cells. On the day prior to treatment, cells were seeded in a glass bottom dish with a density of 1 × 10^5 cells per dish. On the day of treatment, the cells were incubated

with **R-NH$_2$-F127** FONs at a final concentration of 100 μg mL^{-1} for 3 h at 37 °C. Afterwards, the cells were washed for three times with PBS to remove the **R-NH$_2$-F127** FONs and then fixed with 4% paraformaldehyde for 10 min at room temperature. Cell images were taken with a Laser Scanning Confocal Microscope (LCSM) Zesis 710 3-channel (Zesis, Germany) with the excitation wavelengths of 543 nm.

Results and Discussion

The fluorescent dye **R-NH$_2$** is hydrophobic and emits strong crimson fluorescence in solid state. When **R-NH$_2$** is dissolved in THF, it has strong orange fluorescence in dispersed state. After modification by surfactant Pluronic F127, **R-NH$_2$** could be dispersed well in water *via* hydrophilic interaction with F127, meanwhile, the fluorogen was still in aggregated state in the **R-NH$_2$-F127** nanoparticles, and the **R-NH$_2$-F127** composite emitted strong red fluorescence in water with almost the same fluorescent intensity like that in pure THF solution (Fig. 1(a) and 1(b)), which show obvious anti-ACQ property. When the nanoparticles formed, the fluorescent wavelength of the fluorescence dye emerged a 22 nm red-shifted emission. The picture of precipitated **R-NH$_2$** in water was showed in Fig. 1(b) (right), which demonstrated similar emission wavelength like **R-NH$_2$-F127**. The observed spectral shift is attributed presumably to the torsion-locking planarization of the distorted solution geometry of **R-NH$_2$** by aggregation, which narrows the optical bandgap with broadening π-electron conjugation. The appearance of longer-wavelength emission also suggested that close stacking of the planarized **R-NH$_2$** molecules was possibly accompanied with fluorescence-enhancing J-type π-aggregation, often occurring in diarylacrylonitrile derivatives.[23,26] As shown in the inset of Figure 1(a), after surface modification with Pluronic F127, the surfactant modificated nanoparticles **R-NH$_2$-F127** were readily dispersed in water, suggesting the successful formation of hydrophilic FONs.

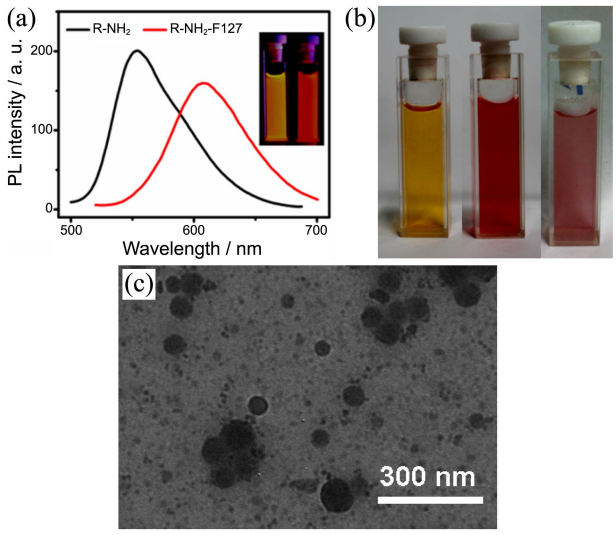

Figure 1. (a) Fluorescence spectra of **R-NH$_2$** in THF and surfactant modificated nanoparticles (**R-NH$_2$-F127**) dispersed in water. Inset: fluorescent image of **R-NH$_2$** in THF and **R-NH$_2$-F127** in water taken at 365 nm UV light; (b) Image of **R-NH$_2$** (left) in THF, **R-NH$_2$-F127** (middle) and R-NH$_2$ (right) in water taken at visible light. (c) TEM image of **R-NH$_2$-F127** FONs dispersed in water, scale bar = 300 nm.

FT-IR spectra showed that a peak centered at 1102 cm^{-1}, which is corresponding to the strecth vibration of C-O, was significantly enhanced in **R-NH$_2$-F127** FONs, demonstrating the successful modification of **R-NH$_2$** dyes with Pluronic F127 (Fig. 2). The transmission electron microscopy (TEM) images further confirmed the formation of FONs. Some small organic spheres with diameters ranging from 40 to 60 nm, which derived from the assembly of **R-NH$_2$** and Pluronic F127 were observed (Fig. 1(c)). The size distribution of **R-NH$_2$-F127** FONs in PBS was tested using a zeta Plus particle size analyzer, showed the size distribution was 116.1 ± 6.9 nm, with a polydispersity index (PDI) of 0.254. The sizes characterized by TEM were somewhat smaller the zeta Plus particle size analyzer likely due to the shrinkage of micelle during the drying process. The formation of such nanostructures is likely due to the strong interactions between the alkyl chain of **R-NH$_2$** and the hydrophobic segments of F127, meanwhile, the hydrophilic segments of Pluronic F127 were covered on the spheres to render them water dis-

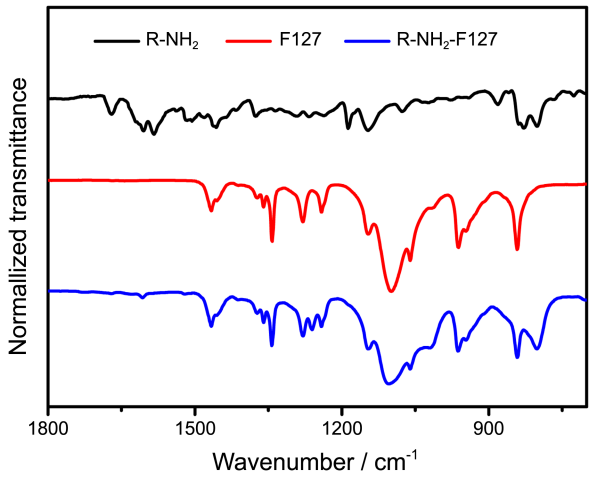

Figure 2. FT-IR spectra of **R-NH$_2$**, F127 and **R-NH$_2$-F127**.

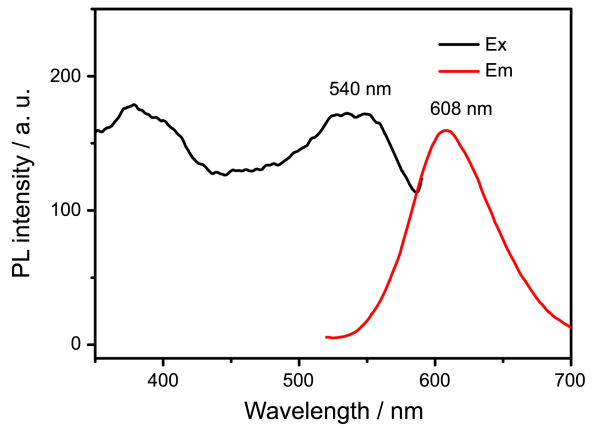

Figure 3. Excitation and emission spectra of **R-NH$_2$-F127** FONs.

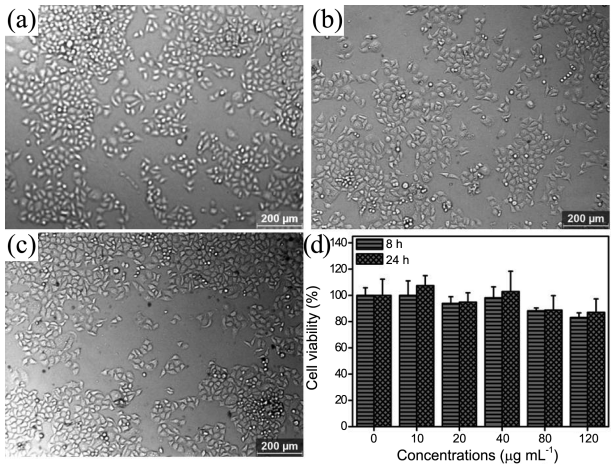

Figure 4. Biocompatibility evaluation of **R-NH$_2$-F127** FONs. (a-c) optical microscopy images of A549 cells incubated with different concentrations of **R-NH$_2$-F127** FONs for 24 h, (a) control cells, (b) 40 μg mL^{-1}, (c) 120 μg mL^{-1}, (d) cell viability of **R-NH$_2$-F127** FONs with A549 cells for 8 and 24 h, respectively. Cell viability was determined by the WST assay.

persible. Taken together, excellent water solubility, small particles, biodegradable potential, and unique photoluminescent (PL) properties (including broad excitation wavelenth and long emission wavelength (Fig. 3)) were found in the red FONs, so we expect that **R-NH$_2$-F127** FONs can be potential used for bioimaging applications.

To test the potential biomedical applications of **R-NH$_2$-F127** FONs, their biocompatibility with A549 cells were subsquently examined.[57-59] Figure 4(a)-(c) showed the microscopy images of cells when they were incubated with different concentrations of **R-NH$_2$-F127** FONs for 24 h, however, no significant cell morphology changes were observed. It could be seen that cells still attached very well to cell plate even the concentration of the FONs was up to 120 μg mL^{-1}. The optical microscopy images implied good biocompatibility of **R-NH$_2$-F127** FONs. Cell viability was further determined to quantitatively evaluate the biocompatibility of **R-NH$_2$-F127** FONs.[60] As shown in Figure 4(d), no obvious cell viability decrease was found when cells were incubated with 40 μg mL^{-1} of **R-NH$_2$-F127** FONs for 8 and 24 h, respectively. The cell viability values were about 90% even the concentration was increased to 120 μg mL^{-1}, further confirming the excellent biocompatibility of **R-NH$_2$-F127** FONs.

The cell imaging applications of **R-NH$_2$-F127** FONs were further explored. The confocal laser scanning microscope (CLSM) images of cells incubated with 100 μg mL^{-1}of **R-NH$_2$-F127** FONs for 3 h were shown in Figure 5.[61-63]

As bright field images (Fig. 5(a)) indicated that cells still kept their normal morphologies, further evidencing the good biocompatibility of **R-NH$_2$-F127** FONs. When cells were excited with 543 nm laser, the cell uptake of **R-NH$_2$-F127** FONs could be clearly distinguished due to they were stained by **R-NH$_2$-F127** FONs. Furthermore, many dark areas which were surrounded by **R-NH$_2$-F127** FONs areas also

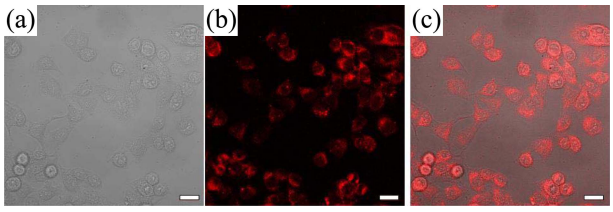

Figure 5. CLSM images of A549 cells incubated with 100 μg mL^{-1} of **R-NH$_2$-F127** FONs for 3 h. (a) bright field, (b) fluorescent image which were excited with 543 nm laser, (c) merged images. Scale bar = 20 μm.

could be found from the CLSM images, which were likely the location of cell nuclues. Therefore, we could expect that the **R-NH$_2$-F127** FONs should be promising candidates for various biomedical applications due to the combined advantages for bio-applications, such as unique PL properties, good water solubility, excellent biocompatibility, and biodegradeble potential.

Conclusion

In summary, a novel strategy for fabrication of red FONs (**R-NH$_2$-F127**) was developed *via* mixing a hydrophobic diarylacrylonitrile derivative conjugated molecule (**R-NH$_2$**) with a commercial surfactant Pluronic F127. These red FONs with diameter ranged from 40 to 60 nm could be facilely obtained and subsquently utilized for cell imaging applications. Our results demonstrated that such red FONs showed remarkable PL properties (anti-ACQ properties and broad excitation wavelength), excellent water solubility and biocompatibility, making them promising for bioimaging applications.

Acknowledgments. Publication cost of this paper was supported by the Korean Chemical Society.

References

1. Weissleder, R.; Pittet, M. J. *Nature* **2008**, *452*, 580.
2. Lee, S.; Cha, E. J.; Park, K.; Lee, S. Y.; Hong, J. K.; Sun, I. C.; Kim, S. Y.; Choi, K.; Kwon, I. C.; Kim, K. *Angew. Chem. Int. Ed.* **2008**, *120*, 2846.
3. Li, L.; Daou, T. J.; Texier, I.; Kim Chi, T. T.; Liem, N. Q.; Reiss, P. *Chem. Mater.* **2009**, *21*, 2422.
4. Wang, F.; Banerjee, D.; Liu, Y.; Chen, X.; Liu, X. *Analyst* **2010**, *135*, 1839.
5. Lin, H. H.; Chan, Y. C.; Chen, J. W.; Chang, C. C. *J. Mater Chem.* **2011**, *21*, 3170.
6. Zhang, X.; Zhang, X.; Tao, L.; Chi, Z.; Xu, J.; Wei, Y. *J. Mater. Chem. B* **2014**, DOI: 10.1039/C4TB00291A.
7. Zhang, X.; Zhang, X.; Yang, B.; Hui, J.; Liu, M.; Wei, Y. *Colloids Surf. B Biointerfaces* **2014**, *116*, 739.
8. Shu, X.; Royant, A.; Lin, M. Z.; Aguilera, T. A.; Lev-Ram, V.; Steinbach, P. A.; Tsien, R. Y. *Science* **2009**, *324*, 804.
9. Michalet, X.; Pinaud, F.; Bentolila, L.; Tsay, J.; Doose, S.; Li, J.; Sundaresan, G.; Wu, A.; Gambhir, S.; Weiss, S. *Science* **2005**, *307*, 538.
10. Hui, J.; Zhang, X.; Zhang, Z.; Wang, S.; Tao, L.; Wei, Y.; Wang, X. *Nanoscale* **2012**, *4*, 6967.

11. Frangioni, J. V. *Curr. Opin. Chem. Biol.* **2003**, *7*, 626.
12. Chandra, S.; Das, P.; Bag, S.; Laha, D.; Pramanik, P. *Nanoscale* **2011**, *3*, 1533.
13. Díez, I.; Ras, R. H. A. *Nanoscale* **2011**, *3*, 1963.
14. Wu, X.; He, X.; Wang, K.; Xie, C.; Zhou, B.; Qing, Z. *Nanoscale* **2010**, *2*, 2244.
15. Resch-Genger, U.; Grabolle, M.; Cavaliere-Jaricot, S.; Nitschke, R.; Nann, T. *Nat. Methods* **2008**, *5*, 763.
16. Cai, Z.; Ye, Z.; Yang, X.; Chang, Y.; Wang, H.; Liu, Y.; Cao, A. *Nanoscale* **2011**, *3*, 1974.
17. Bhirde, A.; Xie, J.; Swierczewska, M.; Chen, X. *Nanoscale* **2011**, *3*, 142.
18. Smith, A. M.; Duan, H.; Mohs, A. M.; Nie, S. *Adv. Drug Deliv. Rev.* **2008**, *60*, 1226.
19. Wang, X.; Xu, S.; Xu, W. *Nanoscale* **2011**, *3*, 4670.
20. Li, K.; Pan, J.; Feng, S. S.; Wu, A. W.; Pu, K. Y.; Liu, Y.; Liu, B. *Adv. Funct. Mater.* **2009**, *19*, 3535.
21. Lin, H. H.; Su, S. Y.; Chang, C. C. *Org. Biomol. Chem.* **2009**, *7*, 2036.
22. Qin, W.; Ding, D.; Liu, J.; Yuan, W. Z.; Hu, Y.; Liu, B.; Tang, B. Z. *Adv. Funct. Mater.* **2010**, *20*, 1413.
23. An, B. K.; Gihm, S. H.; Chung, J. W.; Park, C. R.; Kwon, S. K.; Park, S. Y. *J. Am. Chem. Soc.* **2009**, *131*, 3950.
24. Kumar, M.; George, S. J. *Nanoscale* **2011**, *3*, 2130.
25. Thomas, S. W. I.; Joly, G. D.; Swager, T. M. *Chem. Rev.* **2007**, *107*, 1339.
26. Pu, K. Y.; Li, K.; Shi, J.; Liu, B. *Chem. Mater.* **2009**, *21*, 3816.
27. Zhang, X.; Wang, S.; Xu, L.; Ji, Y.; Feng, L.; Tao, L.; Li, S.; Wei, Y. *Nanoscale* **2012**, *4*, 5581.
28. Liu, J.; Ding, D.; Geng, J.; Liu, B. *Polym. Chem.* **2012**, *3*, 1567.
29. İbrahimova, V.; Ekiz, S.; Gezici, Ö.; Tuncel, D. *Polym. Chem.* **2012**, *2*, 2818.
30. Zhang, X.; Zhang, X.; Wang, S.; Liu, M.; Zhang, Y.; Tao, L.; Wei, Y. *ACS Appl. Mater. Interfaces* **2013**, *5*, 1943.
31. Zhang, X.; Liu, M.; Yang, B.; Zhang, X.; Wei, Y. *Colloids Surf. B Biointerfaces* **2013**, *112*, 81.
32. Luo, J.; Xie, Z.; Lam, J. W. Y.; Cheng, L.; Chen, H.; Qiu, C.; Kwok, H. S.; Zhan, X.; Liu, Y.; Zhu, D.; Tang, B. Z. *Chem. Commun.* **2001**, 1740.
33. Chi, Z.; Zhang, X.; Xu, B.; Zhou, X.; Ma, C.; Zhang, Y.; Liu, S.; Xu, J. *Chem. Soc. Rev.* **2012**, *41*, 3878.
34. Zhang, X.; Chi, Z.; Zhang, Y.; Liu, S.; Xu, J. *J. Mater. Chem. C* **2013**, *1*, 3376.
35. An, B. K.; Kwon, S. K.; Jung, S. D.; Park, S. Y. *J. Am. Chem. Soc.* **2002**, *124*, 14410.
36. Zhang, X.; Liu, M.; Yang, B.; Zhang, X.; Chi, Z.; Liu, S.; Xu, J.; Wei, Y. *Polym. Chem.* **2013**, *4*, 5060.
37. Zhang, X.; Zhang, X.; Yang, B.; Hui, J.; Liu, M.; Chi, Z.; Liu, S.; Xu, J.; Wei, Y. *Polym. Chem.* **2014**, *5*, 318.
38. Zhang, X.; Zhang, X.; Yang, B.; Hui, J.; Liu, M.; Chi, Z.; Liu, S.; Xu, J.; Wei, Y. *Polym. Chem.* **2014**, *5*, 683.
39. Zhang, X.; Zhang, X.; Yang, B.; Hui, J.; Liu, M.; Chi, Z.; Liu, S.; Xu, J.; Wei, Y. *J. Mater. Chem. C* **2014**, *2*, 816.
40. Zhang, X.; Chi, Z.; Li, H.; Xu, B.; Li, X.; Zhou, W.; Liu, S.; Zhang, Y.; Xu, J. *Chem.-Asian J.* **2011**, *6*, 808.
41. Zhang, X.; Chi, Z.; Li, H.; Xu, B.; Li, X.; Liu, S.; Zhang, Y.; Xu, J. *J. Mater. Chem.* **2011**, *21*, 1788.
42. Li, X.; Zhang, X.; Chi, Z.; Chao, X.; Zhou, X.; Zhang, Y.; Liu, S.; Xu, J. *Anal. Methods* **2012**, *4*, 3338.
43. Zhou, X.; Li, H.; Chi, Z.; Zhang, X.; Zhang, J.; Xu, B.; Zhang, Y.; Liu, S.; Xu, J. *New J. Chem.* **2012**, *36*, 685.
44. Zhang, X.; Yang, Z.; Chi, Z.; Chen, M.; Xu, B.; Wang, C.; Liu, S.; Zhang, Y.; Xu, J. *J. Mater. Chem.* **2009**, *20*, 292.
45. Zhang, X.; Chi, Z.; Xu, B.; Li, H.; Yang, Z.; Li, X.; Liu, S.; Zhang, Y.; Xu, J. *Dyes Pigm.* **2011**, *89*, 56.
46. Zhang, X.; Chi, Z.; Xu, B.; Li, H.; Zhou, W.; Li, X.; Zhang, Y.; Liu, S.; Xu, J. *J. Fluoresc.* **2011**, *21*, 133.
47. Li, X.; Chi, Z.; Xu, B.; Li, H.; Zhang, X.; Zhou, W.; Zhang, Y.; Liu, S.; Xu, J. *J. Fluoresc.* **2011**, *21*, 1969.
48. Chen, C.; Liao, J.-Y.; Chi, Z.; Xu, B.; Zhang, X.; Kuang, D.-B.; Zhang, Y.; Liu, S.; Xu, J. *RSC Adv.* **2012**, *2*, 7788.
49. Zhang, X.; Chi, Z.; Xu, B.; Chen, C.; Zhou, X.; Zhang, Y.; Liu, S.; Xu, J. *J. Mater. Chem.* **2012**, *22*, 18505.
50. Zhang, X.; Chi, Z.; Xu, B.; Jiang, L.; Zhou, X.; Zhang, Y.; Liu, S.; Xu, J. *Chem. Commun.* **2012**, *48*, 10895.
51. Zhang, X.; Chi, Z.; Zhou, X.; Liu, S.; Zhang, Y.; Xu, J. *J. Phys. Chem. C* **2012**, *116*, 23629.
52. Zhang, X.; Ma, Z.; Yang, Y.; Zhang, X.; Chi, Z.; Liu, S.; Xu, J.; Jia, X.; Wei, Y. *Tetrahedron* **2014**, *70*, 924.
53. Zhang, X.; Chi, Z.; Zhang, J.; Li, H.; Xu, B.; Li, X.; Liu, S.; Zhang, Y.; Xu, J. *J. Phys. Chem. B* **2011**, *115*, 7606.
54. Yu, Y.; Feng, C.; Hong, Y.; Liu, J.; Chen, S.; Ng, K. M.; Luo, K. Q.; Tang, B. Z. *Adv. Mater.* **2011**, *23*, 3298.
55. Zhang, X.; Zhang, X.; Wang, S.; Liu, M.; Tao, L.; Wei, Y. *Nanoscale* **2013**, *5*, 147.
56. Zhang, X.; Ma, Z.; Liu, M.; Zhang, X.; Jia, X.; Wei, Y. *Tetrahedron* **2013**, *69*, 10552.
57. Zhu, Y.; Li, W.; Li, Q.; Li, Y.; Zhang, X.; Huang, Q. *Carbon* **2009**, *47*, 1351.
58. Li, J.; Zhu, Y.; Li, W.; Zhang, X.; Peng, Y.; Huang, Q. *Biomaterials* **2010**, *31*, 8410.
59. Zhang, X.; Zhang, X.; Yang, B.; Hui, J.; Liu, M.; Liu, W.; Chen, Y.; Wei, Y. *Polym. Chem.* **2014**, *5*, 689.
60. Zhang, X.; Zhang, X.; Yang, B.; Liu, M.; Liu, W.; Chen, Y.; Wei, Y. *Polym. Chem.* **2013**, *4*, 4317.
61. Yang, B.; Zhang, Y.; Zhang, X.; Tao, L.; Li, S.; Wei, Y. *Polym. Chem.* **2012**, *3*, 3235.
62. Zhang, X.; Zhang, X.; Yang, B.; Wang, S.; Liu, M.; Zhang, Y.; Tao, L.; Wei, Y. *RSC Adv.* **2013**, *3*, 9633.
63. Zhang, X.; Zhang, X.; Yang, B.; Liu, M.; Liu, W.; Chen, Y.; Wei, Y. *Polym. Chem.* **2014**, *5*, 399.